Optics Communications 309 (2013) 201–204

Contents lists available at ScienceDirect

Optics Communications

journal homepage: www.elsevier.com/locate/optcom

Circular dichroism in planar extrinsic chirality metamaterial at oblique incident beam

Seoungjun Lee [a,*], Zengbo Wang [a,b], Cheng Feng [c], Jiao Jiao [a], Ashfaq Khan [d], Lin Li [a]

[a] School of Mechanical, Aerospace and Civil Engineering, University of Manchester, Manchester M13 9PL, UK
[b] Schools of Electronic Engineering, Bangor University, Dean Street, Bangor, Gwynedd LL57 1UT, UK
[c] Chemistry Department, University of Leicester, University Road, Leicester LE1 7RH, UK
[d] Department of Mechanical Engineering, NWFP University of Engineering and Technology, Peshawar 25000, Pakistan

ARTICLE INFO

Article history:
Received 3 May 2013
Received in revised form
10 July 2013
Accepted 11 July 2013
Available online 24 July 2013

Keywords:
Metamaterial
Chirality
Circular dichroism
Visible wavelength

ABSTRACT

We present a two dimensional planar extrinsic chirality metamaterial (2D-ECM) design that has strong circular dichroism (CD) in the visible spectrum range rather than usual near-infrared and terahertz range. The 2D-ECM is theoretically investigated by incident beam angles and meta-molecules unit sizes in visible spectrums. Physical mechanism was illustrated in figures of vector directions in electric field.

1. Introduction

Circular dichroism (CD) is characterized by the differential absorption of right circularly polarized (RCP) light and left circularly polarized (LCP) light, and is related to polarization effect which can determine optical activity [1,2]. Circular dichroism spectroscopy has been widely used to gain information about biomolecule, DNA [3–5] and organic compounds [6]. Nanoparticles obtained strong CD in the geometry and composition of a chiral molecule [7–9]. CD was observed in double layers [10], mutually twisted unconnected layers [11], and single-layered gold sawtooth gratings [12] of chiral planar metamaterials at near-infrared wavelengths. Using terahertz frequency, optical activity and coupling effects can generate and assist CD [13,14]. A three-dimensional chiral metamaterial of mutually twisted planar metal patterns generated giant CD in parallel planes due to negative index of refraction [15]. In non-chiral metamaterials, optimized unit cell structure can improve the peak point of CD [16], and elliptical nano-holes array allows to observe CD in visible spectrum [17]. In this paper, we report that two dimensional planar extrinsic chirality metamaterial (2D-ECM) can generate strong CD at visible spectrums using electric distribution of Floquet modes in CST (computer simulation technology) microwave studio software. The structure of the 2D-ECM contains a silver single layer structure on a borosilicate glass substrate. The refractive index and extinction coefficient of silver is changed by wavelengths, and measured at visible wavelengths [18]. The dielectric material of a borosilicate glass (N-BK7) is used for a thick substrate, and the data of the refractive index is obtained [19].

2. Methods

The transmission of RCP and LCP can be mathematically defined in a 2×2 t-matrix as [20]

$$\begin{pmatrix} T_+ \\ T_- \end{pmatrix} = \begin{pmatrix} t_{++} & t_{-+} \\ t_{+-} & t_{--} \end{pmatrix} \begin{pmatrix} I_+ \\ I_- \end{pmatrix} \quad (1)$$

where '+' and '−' are symbols for RCP and LCP incident beams, respectively. The matrix is combined by transmission (T) and incident (I) beam. t_{++} and t_{--} correspond to the transmission amplitude of RCP (I_+) and LCP (I_-) incident beams. t_{+-} and t_{-+} are calculated by the conversion between RCP and LCP. The incident electric field (E^{in}) and transmission electric field (E^{out}) are related to the t-matrix, where LCP and RCP indicate subscripts+and − as defined [20]:

$$E_i^{out} = t_{ij} E_j^{in} \quad (2)$$

and the Circular dichroism (CD) of LCP and RCP is mathematically defined as [20,21]

$$CD = |t_{++}|^2 - |t_{--}|^2 \quad (3)$$

* Corresponding author. Tel.: +44 161 306 3816.
E-mail address: seoungjun.lee@postgrad.manchester.ac.uk (S. Lee).

0030-4018/$ - see front matter
http://dx.doi.org/10.1016/j.optcom.2013.07.033

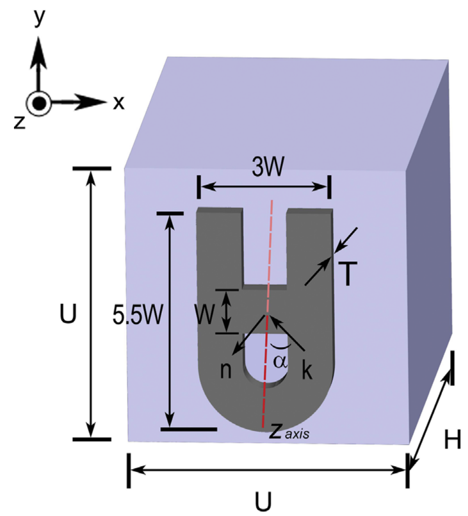

Fig. 1. Asymmetric unit cell structure (U=250 nm) of a borosilicate glass substrate (H=1000 nm) and silver unit cells (T=20 nm and W=40 nm). n is the direction of vector perpendicular to the unit cell. k is the direction of the incident beam, and emits along the relative x axis. α is angle of the incident beam, and is calculated by the direction of incident beam k to z axis.

$$CD = |T_{LCP}| - |T_{RCP}| \tag{4}$$

CD spectrum was simulated by modern finite integrate technique (FIT) in frequency domain. Different angles of oblique incident beams were applied in the unit cell. The spectrum was demonstrated and compared between LCP and RCP. The 2D-ECM design consists of unit cells of 20 nm thick silver layer on a 1000 nm thick borosilicate glass substrate as shown in Fig. 1. The borosilicate glass substrate is dielectric substrate which can help to break mirror symmetry so optical activity can be boosted [22]. At vertical incident beam (α=0°), it forms mirror image because the asymmetric unit cell structure has the same direction as incident beam so it is not 3D-chiral. However, at tilted incident beam ($\alpha \neq 0°$), the asymmetric unit cell structure is transformed into extrinsically 3D-chiral as it is not mirror image between LCP and RCP [13]. The 2D-ECM forms unit cell boundary condition in x and y dimensions, and open boundary condition in z dimension. The unit cell boundary condition is quite similar to the periodic boundary condition but when open boundaries are perpendicular such as using waveguide ports, the unit cell boundary condition approaches Floquet modes. Oblique incident beams of LCP and RCP propagates into z dimension using waveguide ports. The waveguide ports support to calculate returning power using S-parameters.

3. Results and discussion

Fig. 2 shows CD spectrum of the 250 nm unit cell in wavelengths between 450 nm and 800 nm at various incident angles of α=0°, ±20°, ±71° and ±80°. In wavelengths below 610 nm, the spectrum curves are highly oscillating. This is because of strong optical diffraction associated with the unit cell [20], which may lead to disturbance and diffraction of the oblique incident beams in the layer of the unit cell. Above 610 nm wavelengths, the spectrum curves change smoothly because the optical diffraction is negligible. The maximum CD peaks were 0.4914 at 726.39 nm visible wavelength occurring at angles α=71°, where is the highest difference between LCP and RCP. It shows that 71° tiled incident beams of LCP and RCP may have distinctive interactions between electric and magnetic dipoles, which may generate most clear optical activity. CD did not appear at 0° oblique incident beams because the projection of electric and magnetic moment is symmetrically the same between LCP and RCP [23]. It means that the location and magnitude of electric and magnetic dipoles could be the same. The ±20°, ±71° and ±80° were intersected

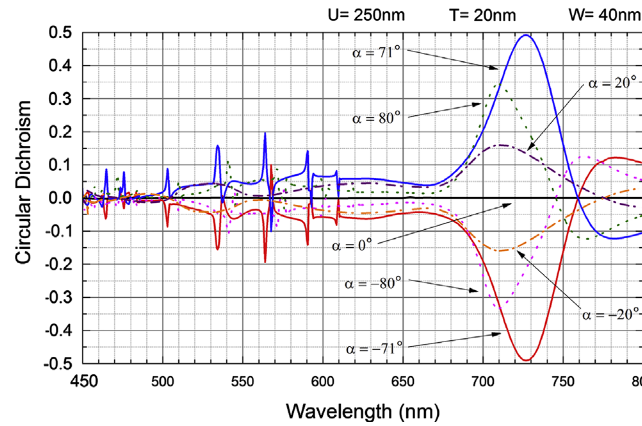

Fig. 2. Comparison of CD in the 250 nm unit cell between different incident beam angles as α= ±80°, ±71°, ±20° and 0° at wavelengths (λ) between 450 nm and 800 nm. The maximum CDs are in Table 1.

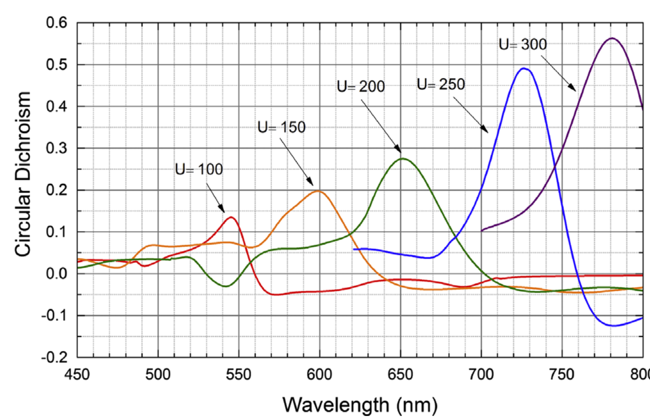

Fig. 3. Dependence of CD on the wavelengths (λ) between 450 nm and 800 nm for 100 nm unit cell with α=77°, 150 nm unit cell with α=58°, 200 nm unit cell with α=45°, 250 nm unit cell with α=71°, and 300 nm unit cell with α=57°. The maximum CDs are in Table 2. Highly oscillated curves are removed in U=250 and 300.

Table 1
aaaaa250 nm unit cell with various angles, wavelengths and CD.

Angle (α, deg)	Optimized wavelength (λ, nm)	Transmission spectrum (CD)
0	It does not appear	It does not appear
20	710.90	0.1602
71	726.36	0.4914
80	710.06	0.3438

Table 2
Different sizes of unit cells with optimized angles, wavelengths and CD.

Unit cell size (U, nm)	Optimized angle (α, deg)	Optimized wavelength (λ, nm)	Transmission spectrum (CD)
100	77	545.45	0.1345
150	58	598.80	0.1976
200	45	651.47	0.2750
250	71	726.36	0.4914
300	57	781.25	0.5627